OLIVE LEAVES EXTRACT AS GREEN CORROSION INHIBITOR FOR β-BRASS ALLOY IN ACIDIC MEDIUM

Balsam Mohammed and Taghried A. Salman*

*Department of Chemistry, College of Science, Al-Nahrain University, Baghdad, Iraq.

Abstract

Olive leaves have been extracted in aqueous media, the extract was characterized using Furrier transformed infrared spectroscopy (FTIR) and gas chromatography interfaced with mass spectroscopy (GC-MS). Results showed that extract contain large numbers of organic compounds. The inhibition effect of olives leaves extract (OLE) on the corrosion of β-brass in 1M H_2SO_4 at temperature range from 293 to 313 K was studied using weight loss and Tafel polarization techniques. Inhibition efficiency data were increases with increasing the extract concentration and decreases as the temperature increase. The extract shows the highest inhibition efficiency at 400 ppm, 81.54%. Tafel polarization measurements relive that OLE acts as mixed type inhibitor. The adsorption of studied extract on β-brass surface follows the Langmuir adsorption isotherm. In the presence of the extract, scanning electron microscope image shows a smother surface for β-brass in the presence of the OLE. The adsorption energies data also agree with the experimental inhibition efficiency trend.

Key words: Corrosion inhibition; β-brass; acidic solution; Polarization; olive leaves.

Introduction

Cu-Zn alloys, also known as brass, are the most representative Cu-based alloys that are popular in modern industry. The addition of Zn into Cu leads to a significant improvement of mechanical properties of Cu alloys. However, Zn is less noble than Cu, leading to a selective leaching of Zn from Cu-Zn alloys, *i.e.*, dezincification. Dezincification is the most annoying problem that hinders the utilization of brass in water plumbing, heat exchange engineering and marine engineering. During the past decades, numerous investigations have been focused on the mechanistic explanation of dezincification and its inhibition. Especially in the case of neutral environment leads to the formation of oxide scale, the release of cations and the simultaneous formation of a Zn depleted Cu rich layer which complicate the corrosion process. A member of the copper-zinc alloys is β-brass, it is widely used in many applications in electronic industries and communications as a conductor in electrical power lines, pipelines for domestic and industrial water utilities including sea water, heat conductors and heat exchangers (Al-Mobarak *et al.,* 2010). This alloy is, however, like many others, subject to adverse corrosive environmental degradation challenges in service and this threatens its

engineering performance, for example sulfuric acid contributes to the corrosion of metal surface which is widely used for pickling, cleaning, descaling and etching of metals (Ghulamullah *et al.,* 2015). Preventing corrosion of metals to the greatest possible extent is of extreme importance. One of the most efficient and economical ways of achieving this is by using inhibitors, chemical substance which when added to the corrosive environment at an optimum concentration decreases the corrosion rate of metals or alloys (Mostafa *et al.,* 2012). Organic compounds containing hetero-atoms (N, S, O), which are one of the main requisites for the inhibitory action (Milan *et al.,* 2013), However, the application of these compounds can be limited due to their toxicity, and non-biodegradable. In very recent time, there has been wide interest among researchers in the use of plant peels extracts as green corrosion inhibitors for the corrosion of metals/alloys. In many cases, the corrosion inhibitive effect of some plants extracts has been attributed to the presence of tannin and polyphenols in their complex chemical constituents (Cleophas *et al.,* 2016).

The present work aims to study the inhibitory effect of natural olive leaves extract for β-brass corrosion in 1M H_2SO_4 by using weight loss and Tafel polarization techniques. The influence of inhibitor concentration and

***Author for correspondence :** E-mail : dr.tag_s@yahoo.com

the role of temperature were also investigated. The organic species present in the extract were characterized by high performance gas chromatography and Fourier transform spectroscopy.

Materials and methods

Preparation of Electrodes and electrolytes

β-brass working electrodes were obtained from a local metal market in Baghdad. It composed of 55% Cu and 45% Zn. A cylindrical brass alloy sample was cut into average size of 1.2mm × 2cm coupons for weight loss and potentiostatic polarization measurements. All samples surfaces were polished using series of different grades of emery paper (320, 500, 1000, 2400, 4000) sprayed with diamond product that contain ethanol with different size of diamond particles (1, 3, 6, 9) µm to obtained a mirror finish, the specimen then rinsed with distilled water and degreased with acetone. 1M of H_2SO_4 solution used as aggressive medium was prepared with 98% of stock analytical grade H_2SO_4 and distilled water.

The influence of the olive leaf extract concentration was studied at various temperatures in the range 293-318 K. A thermostat controlled the temperature with an accuracy of ±0.5°C.

Extraction solution and extract preparation

Fresh olive leaves were collected from different part of the olive tree then extensively washed under running tape water followed by washing with sterilized distilled water. They were further air-dried at room temperature, powdered with the help electric grinder and then sieved using a (75µm × 20cm) sieve. The dry powder was further

extracted by using aqueous solvent. 100 g of powder was mixed with 100 ml sterilized distilled water and kept at room temperature for 24h on an orbital shaker with 150 rpm. The solution was filtered using muslin cloth; after that, the filtrate was centrifuged at 5000 rpm for 15 min. The supernatant thus obtained was filtered through Whitman's filter No.1, after that filtrate was evaporated. The solid residue was collected and used in preparation of different concentration of 100, 200, 300 and 400 ppm in sulphuric acid solution.

Fourier transform infrared spectroscopy

The OLE powder was subjected for FTIR spectroscopy (Shimadzu, IR Affinity 1, Japan) with scan range between 4000-500 1/cm.

Characterization of the olive leaf extract by GC-MS Chromatography

The olive leaves extract was prepared by dissolve 3 g of it in 30 ml of methanol and left for 3 days so that all organic compounds dissolve. After that the mixture was filtered using filter paper. GC-MS that used for analysis was made (QP 2010 Plus SHIMADZU, Japan) computerized control. The measurement began with inject of 2 µL using micro syringe at 70 eV using Helium as inert gas. The run time of the entire experiment was 30 min. Each compound was quantified in comparison with its standard when it was available while the other detected compounds were quantified by other equivalent compounds.

Weight loss measurements

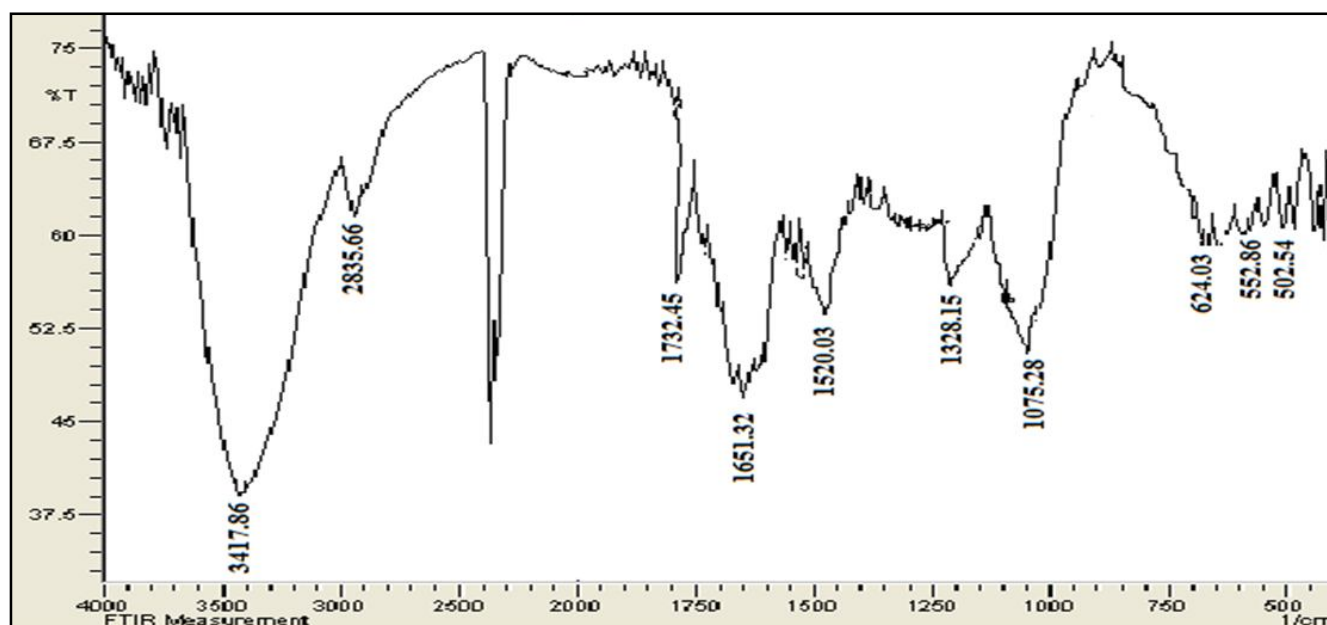The used β–brass specimens have a circular form

Fig. 1: FTIR spectrum for olives leaves extract.

with surface area of 2.5 cm². The immersion time for weight loss experiment was 24 h at various temperature range from 293 to 313 K. After the immersion period, the specimens were cleaned according to ASTM G-81, and reweighed to 10^{-4} g to determine the corrosion rate (Sudhish *et al.,* 2012 and Alaoui *et al.,* 2016). However, weight loss allows us to calculate the mean corrosion rate, as expressed in mg cm^{-2} h^{-1}. The inhibition efficiency, *IE*w%, is determined as follows:

$$IE_W\% = (C_R^o - C_R) / C_R$$

where C_R^o and C_R are, respectively, the rates of β–brass corrosion without and with the presence of inhibitor.

Potentiostatic polarization experiments

Potentiostatic polarization experiments were performed on the mounted specimens present in the sulphuric acid media without and with OLE inhibitor. For test, 1 cm² surface area of the specimen was exposed to the test solution. The experiments were performed using a polarization cell with a three – electrode system consisting of a reference electrode (saturated calomel electrode), a working electrode (β- brass); and platinum electrode was used as axillary electrode. The polarization cell was connected to a potentiostat and interfaced with a computer for data attainment and analysis. The potentiodynamic studies were made at a scan rate of 2 mV/s from (±200) mv and the polarization curves were recorded in order to determine the electrochemical parameters.

Results and discussion

Fourier transform infrared spectroscopy of OLE

The olive leaves extract contain organic compounds, and these compounds were adsorbed on the β-brass surface providing protection against corrosion. FTIR spectra was carried out to identify the adsorbed extract on the β-brass surface. The spectrum is shown in Fig 1.

Olive leaves extract show a number of absorption peaks, reflecting its complex nature. A peak at 3417 and 1732 cm^{-1} in OLE were characteristic of the O–H and C=O stretching modes for the hydroxyl and carbonyl groups possibly presents in oleuropein and other active compounds present in the olive leaf extract (Quraishi *et al.,* 2000, El-Etre, 2007 and Mostafa *et al.,* 2014). The absorption peak at 2835 cm^{-1} indicates to –CH stretching vibrations of –CH$_3$ and –CH$_2$ functional groups. The shoulder peak at 1732 cm^{-1} assigned to C=O carboxylic acid group. On the other hand, The IR bands shown at The peak at 1604 cm^{-1} indicated the fingerprint region of CO, C–O and O–H groups, which exists as functional groups of olive leaves extract. The absorption peaks at 1604 cm^{-1} could be attributed to the presence of C–O stretching in carboxyl coupled to the amide linkage in amide I. The band at 1520 cm^{-1} was characteristic of amide II arises as a result of the N-H stretching modes of vibration in the amide linkage. The band at 1328 cm^{-1} assigned to the methylene scissoring vibrations from the protein. The peak at 1075 cm^{-1} are attributable to vibration of C–O ether and ester groups in the compounds of olive leaf extract (Zainab *et al.,* 2016).

Active compounds contents of the studied olive leaf extract

The GC-MS chromatogram Fig. 2 shows several peaks corresponding to the compounds presents in the olive leaves extract. The most abundant compound was oleuropein. The main active compounds presents in OLE are tabulated in table 1.The results obtained were previously proven (Gordana *et al.,* 2016).

Weight loss measurements

The corrosion rate of β–brass in 1M H$_2$SO$_4$, without and with various concentrations of OLE, was determined after 24 h of brass immersion at different temperatures in the range from 293 to 313 K. The obtained
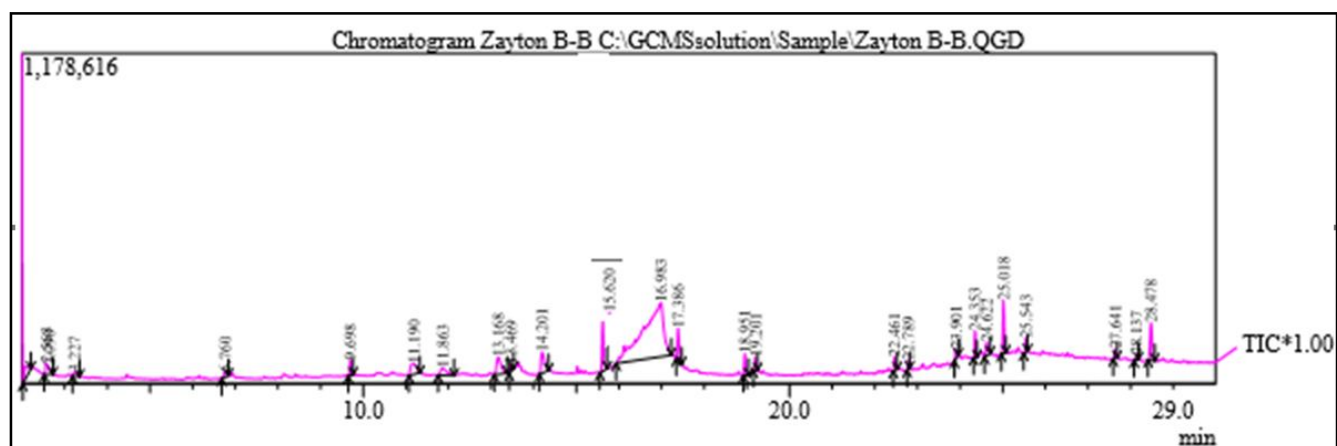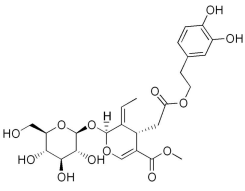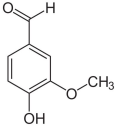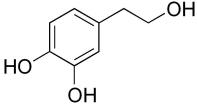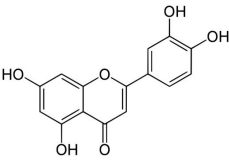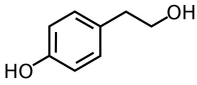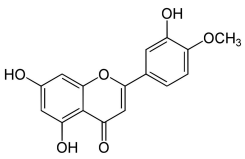

Fig. 2: Chromatogram of extract of OLE.

Table 1: The main active compounds in olive leaves extract.

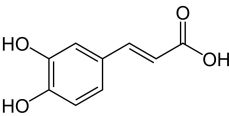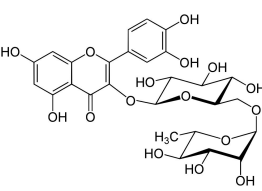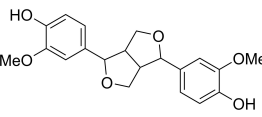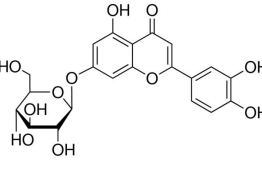| No.	Name of Compounds	Chemical formula	M.Wt (g/mol)	Chemical Structures
1	oleuropein	$C_{25}H_{32}O_{13}$	540.510	
2	vanillin	$C_8H_8O_3$	152.149	
3	hydroxytyrosol	$C_8H_{10}O_3$	154.165	
4	Luteolin	$C_{15}H_{10}O_6$	286.240	
5	Tyrosol	$C_{10}H_8O_2$	138.164	
6	Diosmetin	$C_{16}H_{12}O_6$	300.260	
7	Caffeic acid	$C_9H_8O_4$	180.160	
8	Rutin	$C_{27}H_{30}O_{16}$	610.521	
9	Pinoresinol	$C_{20}H_{22}O_6$	358.380	
10	Luteolin-7-glucoside	$C_{21}H_{20}O_{11}$	448.370	

experimental data are presented in table 2. It has been observed that the inhibition efficiency increased with the concentration of OLE, reaching a maximum at 400 ppm of OLE. This behavior could be attributed to the increase in adsorption of the inhibitor at the metal/solution interface when its concentration is increased. AS well as, the electron donating groups increase the inhibition efficiency of the inhibitor. On the other hand, an increase of temperature resulted on a decrease in corrosion protection.

Electrochemical polarization studies

Polarization behavior of β-brass in 1M H_2SO_4 in the presence and absence of different concentrations of OLE (100, 200, 300 ,400) ppm at temperature range between 293 to 313 K is shown in Fig. 3. Electrochemical kinetic parameters obtained from polarization curves by potentiodynamic technique are shown in table 3.

Data presented in table 1 indicates that the corrosion potential values in the absence and presence of the inhibitor randomly variable in all inhibitor concentrations and temperatures, anodic and cathodic Tafel slopes (b_a, b_c) are more or less constant. Furthermore, presence of OLE decreases the corrosion current densities and this decrease is more noticeable with an increase of the inhibitor concentration. Fig. 4 show that OLE inhibits both anodic and cathodic reactions, so it's considered to be mixed type inhibitor (Gordana *et al.,* 2016).

The inhibition efficiency (IE) of the olive leaves extract was calculated using the following relation:-

$$IE\ (\%) = [\ (\ i^o_{corr.} - i^{inh.}_{corr.})\ /\ i^o_{corr.}]\ \times 100$$

where $i^o_{corr.}$ and $i^{inh.}_{corr.}$ are respectively, the corrosion current densities in the absence and presence of OLE as inhibitor. The current densities ($i_{corr.}$) values were calculated using Tafel extrapolation method. Both Tafel lines were extrapolated until they intersected at $E_{corr.}$. Alternatively, surface coverage (θ) was determined as θ = (% IE/100). The relevant parameters obtained from the above relations are presented in table 1. From the results given in table it can be seen that inhibition effecinces increase with increasing the inhibtor concentration and decreases as the temperature increased. The highest inhibitor efficiency of 81.54% was achieved at 400 ppm. The inhibition efficiencies,

calculated from Tafel polarization results, showed the same trend as those obtained from weight loss measurements.

Effect of temperature and activation studies

Thermodynamic corrosion parameters, namely activation energy E_a, entropy $\Delta S^{\#}$ and enthalpy $\Delta H^{\#}$ of activation, were calculated using Arrhenius equation and its alternative formulation called transition state equation(Taghried *et al.*, 2019).
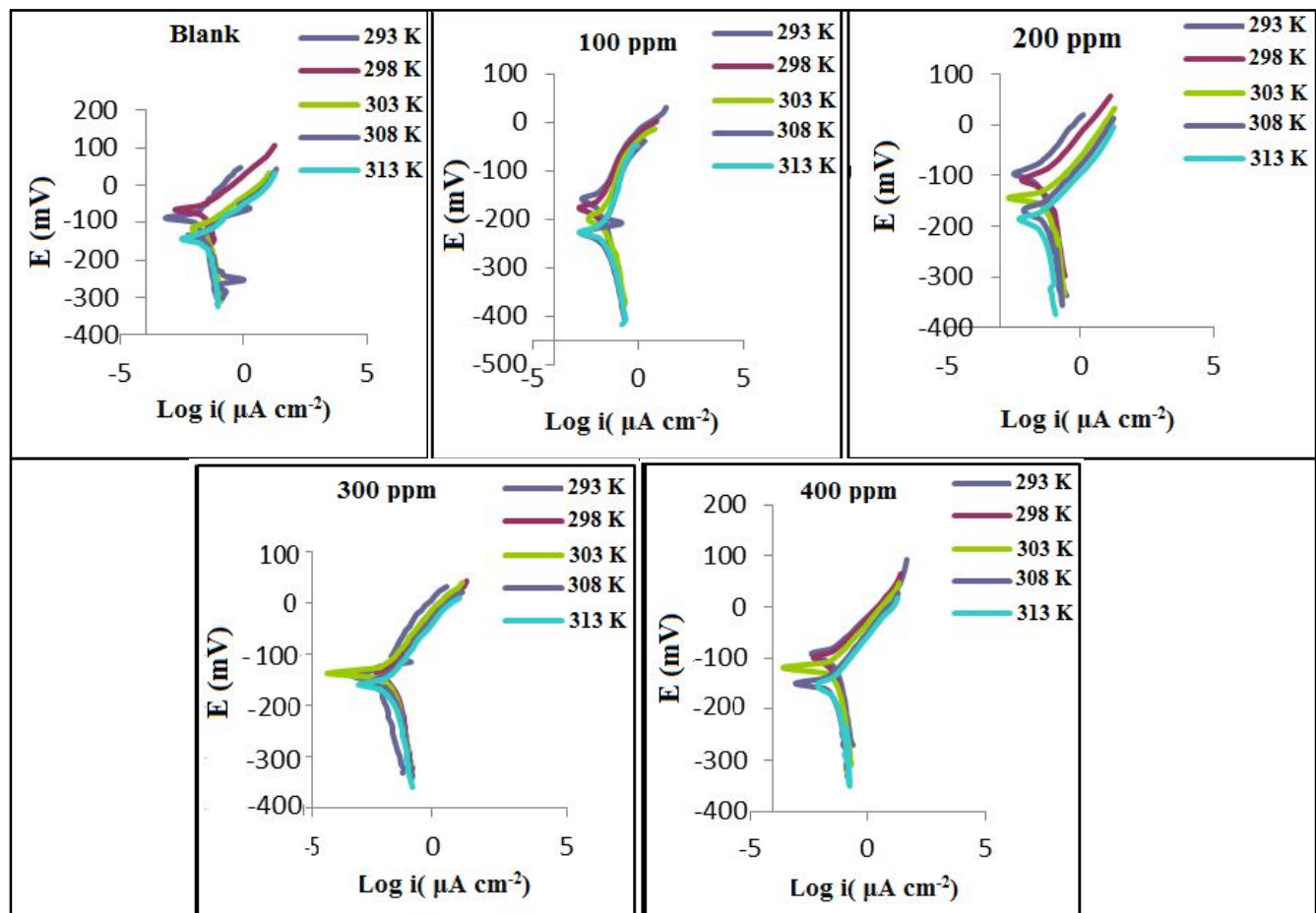
$$\log i_{corr.} = \log A - \frac{E_a}{2.303RT}$$

$$i_{corr.} = \frac{RT}{Nh} \exp\left(\frac{\Delta S^{\#}}{R}\right) \exp\left(-\frac{\Delta H^{\#}}{RT}\right)$$

Where T is the absolute temperature, R is the universal gas constant, h is Plank's constant, N is Avogadro's number. Fig. 4 illustrate Arrhenius relations and the obtained activation parameters for adsorption of OLE on β-brass surface at different conditions are shown in table 4.

The results showed that the activation energy significantly increases in the presence of the inhibitor. This can attributed to the fact that the inhibitor species are adsorbed on the brass surface. Positive sign for $\Delta H^{\#}$, reflecting

Table 2: Corrosion rates and inhibition efficiencies of β – brass in 1M H_2SO_4, in the absence and presence of different concentrations OLE at various temperatures in the range (293-313) K after 24 h of immersion.

blank		T(K)		293	298	303	308	313	
		CR (g/m² d)		6.77	7.07	13.00	17.30	21.10	
Inhibitor		**100 ppm**		**200 ppm**		**300 ppm**		**400 ppm**	
	T (K)	CR (g/m² d)	IE%	CR (g/m² d)	IE%	CR (g/m² d)	IE%	CR (g/m² d)	IE%
	293	3.15	53.47	2.54	62.48	1.90	71.90	1.25	81.53
	298	3.45	51.20	3.12	55.87	2.31	67.33	1.74	75.36
	303	6.78	47.85	6.18	52.46	5.03	61.31	3.91	69.92
	308	9.36	45.89	8.51	50.81	7.75	55.20	6.53	62.25
	313	12.28	41.80	11.32	46.35	10.33	51.05	8.61	59.19

Fig. 3: Polarization curves of β-brass corrosion in 1M H_2SO_4 in the absence and presence of different concentrations OLE at various temperatures in the range (293-313) K.

Table 3: Corrosion parameters of β-brass corrosion in 1M H$_2$SO$_4$ in the absence and presence of different concentrations OLE at various temperatures in the range (293-313) K.

Inhibitor conc. [ppm]	T (K)	-E$_{corr}$ (mV)	i$_{corr}$ (µA/ cm^2)	Tafel slope (mV/dec) -b$_c$	+b$_a$	IE%	θ
0	293	103.0	23.78	196	43.9	-	-
	298	151.3	24.86	157.3	53.9	-	-
	303	159.3	45.75	160.9	70.6	-	-
	308	189.1	56.33	126.0	68.90		-
	313	182.8	65.67	229.1	73.50	-	-
100	293	158.7	11.08	249.6	89.60	53.41	0.534
	298	186.5	12.31	142.7	74.80	51.21	0.512
	303	212.0	23.89	189.4	60.10	47.78	0.477
	308	229.9	30.50	204.0	72.90	45.85	0.458
	313	238.2	38.22	185.6	61.20	41.80	0.418
200	293	110.4	8.89	116.5	61.80	62.41	0.624
	298	147.7	10.93	140.1	72.00	55.91	0.559
	303	165.9	21.75	227.7	60.50	52.46	0.524
	308	179.9	27.69	151.6	62.90	50.84	0.508
	313	196.2	35.21	297.9	74.20	46.38	0.463
300	293	154.5	6.68	166.5	68.30	71.91	0.719
	298	140.1	8.12	168.8	75.60	67.34	0.673
	303	147.2	18.90	141.0	70.70	61.36	0.613
	308	166.7	25.23	268.1	85.70	55.21	0.552
	313	170.6	32.12	363.6	96.80	51.09	0.519
400	293	98.6	4.39	104.8	62.20	81.54	0.815
	298	111.3	6.18	159.8	89.50	75.38	0.753
	303	130.0	13.77	109.6	74.10	69.90	0.699
	308	147.6	21.27	199.4	119.4	62.24	0.622
	313	153.8	26.81	226.7	116.4	59.17	0.591

the endothermic nature of corrosion process. The negative values of ΔS$^{\#}$ pointed to a greater order produced during the process of activation. This can be achieved by the formation of activated complex and represents association or fixation with consequent loss in the degrees of freedom of the system during the process(Khadom *et al.,* 2009).

Adsorption isotherm studies

Basic information about the interaction between the inhibitor molecules and β-Brass surface can be provided by the adsorption isotherm. In the range of studied temperature, correlation between the extract concentration and surface coverage was obtained using Langmuir adsorption isotherm that given as

$$K_{ads.}\ C = \theta/(1-\theta)$$

Where K$_{ads.}$ is the equilibrium constant for the inhibitor adsorption process and C is the concentration of the inhibitor. The linear regressions between C/θ and C for each temperature over concentration range (100–400) ppm are shown in Fig. 5a and the adsorption parameters are listed in table 5. The results obtained show very high correlation coefficients and the slopes values are close to one. These finding confirm that the adsorption of the inhibitor molecules in 1M H$_2$SO$_4$ solution follows Langmuir adsorption isotherm.

The values of K$_{ads}$ were calculated from the intercepts of the straight lines on the C/θ – axis. The K$_{ads}$ was related to the standard free energy of adsorption, ΔG$^{o}_{ads}$ according to the following equation:

$$K_{ads.} = (1/55.5)\ exp\ [(-\Delta G_{ads.})/RT]$$

R is the universal gas constant, T is the absolute temperature (K) and the constant value 55.5 represents
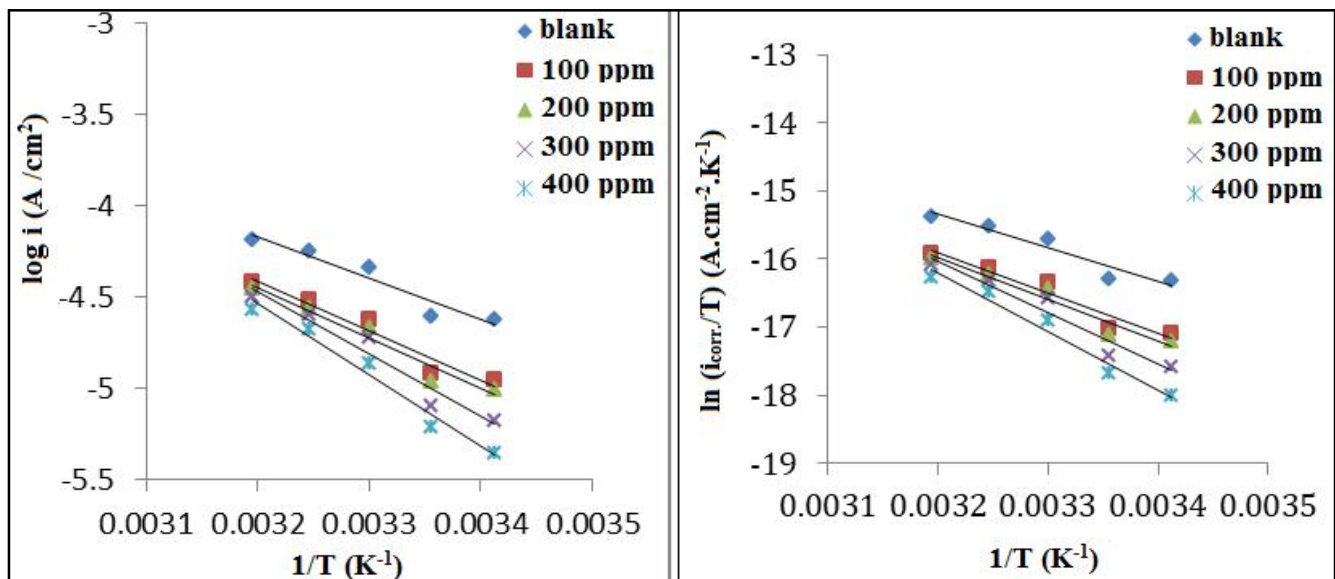
Fig. 4: Arrhenius plots of log *i*$_{corr}$ versus 1/T for the corrosion of β-brass in H$_2$SO$_4$ solution in the absence and presence of different concentrations OLE at various temperatures in the range (293-313) K.

Table 4: Activation energy (E_a), activation enthalpy (ΔH^*), and the entropy of activation (ΔS^*) of β-brass corrosion in 1 M H_2SO_4 solution in the absence and presence of different concentrations OLE at various temperatures in the range (293-313) K.

OLE Conc. (ppm)	E_a (kJ. mol^{-1})	A(mole cules. cm^{-2}.s^{-1})	ΔH^* (kJ. mol^{-1})	$-\Delta S^*$ (J.K^{-1}. mol^{-1})
-	43.48316	7.60×10^{26}	40.96308	193.985
100	51.85046	1.09×10^{28}	49.32696	171.828
200	52.9227	1.52×10^{28}	50.40778	169.085
300	65.29175	1.68×10^{30}	63.17809	129.942
400	74.17603	4.34×10^{31}	71.64174	102.922

Table 5: Thermodynamic parameters for adsorption of the OLE on the surface of β–brass alloy in 1M H_2SO_4 solution.

T(K)	K_{ads} (M^{-1})	$-\Delta G_{ads}$ (kJ.mol^{-1})	$-\Delta H_{ads}$ (kJ.mol^{-1})	ΔS_{ads} (J.K^{-1}.mol^{-1})
293	8833.92	38.96		
298	9523.81	39.81		
303	8771.93	40.27	23.62	21.24
308	10695.19	41.44		
313	17921.15	43.46		

the concentration of water in solution in mol/dm^3. The enthalpy of adsorption ($\Delta H_{ads.}$) and entropy of adsorption ($\Delta S_{ads.}$) have been calculated by plotting the $\Delta G_{ads.}$ data against temperature for molar sulphuric acid solution in the presence of OLE inhibitor at various concentrations as shown in Fig. 5b by using the following equation.
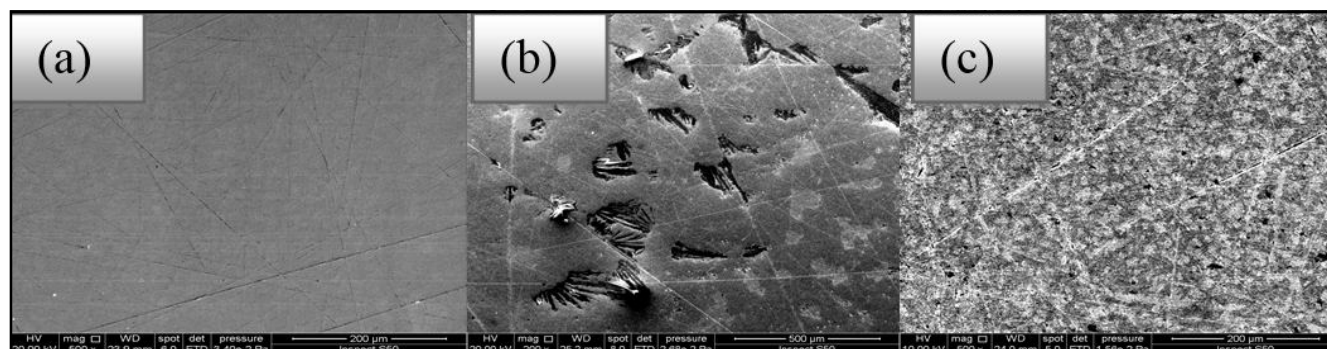
$$\Delta G_{ads.} = \Delta H_{ads.} - T\Delta S_{ads.}$$
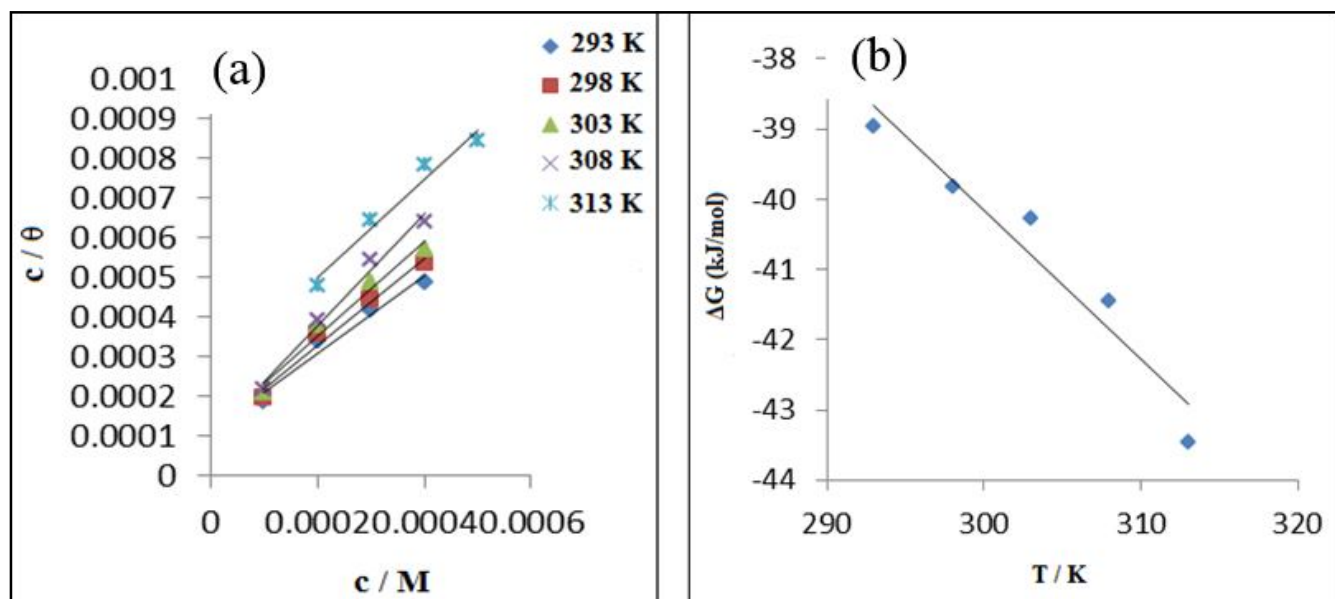
The results show that the average value of standard adsorption free energy $\Delta G_{ads.}$ equal -33.34 kJ.mol^{-1}. The negative values of $\Delta G_{ads.}$ refers to the spontaneity of the adsorption process and stability of the adsorbed layer on the brass surface. Researchers (Khamis *et al.,* 2013 and Mohamed *et al.,* 2015)[15,16] suggested that the range of ΔG_{ads} of chemical adsorption processes for organic inhibitor in aqueous media lies around -40 kJ.mol^{-1} Therefore, for the present work the value of "Gads has been considered within the range of chemical adsorption. The values obtained of ΔH_{ads} confirm the exothermic behavior of the adsorption process of OLE on the β–Brass surface in sulphuric acid solution. While an endothermic adsorption process ($\Delta H_{ads.} > 0$) is attributed unequivocally to chemisorption[16]. The positive sign of $\Delta S_{ads.}$ values indicates the increase in randomness.

SEM Results

SEM analysis was carried out to visualize the composition of the films formed on the alloys surfaces immersed in the aggressive solution without and with 400 ppm of OLE. Fig. 6 a, b and c show, respectively, the SEM images for polished β-Brass alloy, without and with inhibitor after 24 h immersion period. Fig. 6b shows a rougher surface obtained in uninhibited solution compared to surface obtained in the presence of OLE Fig. 6c that seems smooth surface with a fine texture. These observations confirming the existence of the protective film formed on brass surface (Priyanka *et al.,* 2016).

Conclusions

Olive leaves extract has been confirmed as a good corrosion inhibitor for β-brass in 1 M H_2SO_4 solution.

Fig. 5: a- Langmuir isotherm plots for adsorption of OLE on β-brass surface in 1M H_2SO_4 solution, b- The variation of Gibbs free energies ($\Delta G_{ads.}$) with temperature.

Fig. 6: Scanning electron micrographs of β-brass (a): bare polished alloy (b): after immersion 24h in 1M H_2SO_4 solution (c): after immersion 24h in 1M H_2SO_4 and in presence of 400 ppm of OLE.

The presence of OLE promotes the formation of protective layer on β-brass surface. The inhibiting species present in the olive leaf extract act as a mixed type inhibitor adsorbed on the brass surface. The adsorption of extract on steel surface is a spontaneous process and follows Langmuir adsorption isotherm. The decrease of the inhibition efficiency with the temperature and the value obtained for the activation energy of the corrosion process indicate a predominant chemisorption mechanism. Such type of inhibitors is efficient at ambient temperature, but is characterized by a loss in inhibition efficiency at elevated temperatures. Reasonably good agreement was observed between the obtained inhibition efficiencies values from weight loss and Tafel polarization techniques.

References

Al-Mobarak, N.A., K.F. Khaled, O.A. Elhabib and K.M. Abdel-Azim (2010). Electrochemical investigation of corrosion and corrosion inhibition of copper in NaCl solutions, *J. Mater. Environ. Sci.,* **1(1):** 9-19.

Alaoui, K., Y. El Kacimi and M. Galai (2016). Anti-corrosive properties of Polyvinyl-Alcohol for carbon steel in hydrochloric acid media: Electrochemical and thermodynamic investigation *J. Mater. Environ. Sci.,* **7(7):** 2389-2489.

Cleophas, A.L., T.L. Rol and O. Ohwofasa (2016). Effect of *Allium sativum* Extracts on the Corrosion and Inhibition of á- Brass in HCl, *Mor. J. Chem.,* **4:** 711-721.

El-Etre, A.Y. (2007). Inhibition of acid corrosion of carbon steel using aqueous extract of olive leaves *J. Colloid Interface Sci.,* **314:** 578-583.

Ghulamullah, K., S. Md., J.B. Kazi, B.M. Wan, L.F. Hapipah, M. Fadhil and Kh. Ghulam (2015). Application of Natural Product Extracts as Green Corrosion Inhibitors for Metals and Alloys in Acid Pickling Processes- A review, *Int. J. Electrochem. Sci.,* **10:** 6120-6134.

Gordana, P., K. Frankica and V. Želimir (2016). Olive Leaf Extract as a Corrosion Inhibitor of Carbon Steel in CO_2-Saturated Chloride–Carbonate Solution, *Int. J. Electrochem. Sci.,* **11:** 7811-7829.

Khadom, A.A.A.S. Yaro, A.S. AlTaie and A.H. Kadum (2009). Electrochemical, Activations and Adsorption Studies for the Corrosion Inhibition of Low Carbon Steel in Acidic Med, *Port. Electrochimica Acta,* **27(6):** 699-712.

Khamis, A., M.S. Mahmoud, I.A. Mohamed and B.E. El-Anadouti (2013). Enhancing the inhibition action of cationic surfactant with sodium halides for mild steel in 0.5M H_2SO_4, *Corros. Sci.,* **74:** 83-91.

Milan B.R., B.P. Marija, T.S. Ana, M.M. Snežana and M.A. Milan (2013). Cysteine as a green corrosion inhibitor for Cu37Zn brass in neutral and weakly alkaline sulphate solutions, *Environ. Sci. Pollut. Res.,* **20:** 4370-4381.

Mostafa, M. Kh., H.I. Eman and El. Fatma (2012). Biosynthesis of Au nanoparticles usimg olive leaf extract:1 st nano updates, *Arab. J. Chem.,* **5:** 431-437.

Mostafa, MH. Kh., H.I. Eman, Z. EL-B. Khalid and M. Doaa (2014). Green synthesis of silver nanoparticles using olive leaf extract and its antibacterial activity, *Arab. J. Chem.,* **7(6):** 1131-1139.

Mohamed, H., A.Y. El-Etre and K.M. Berry (2015). Novel inhibitors for carbon steel pipelines corrosion during acidizing of oil and gas wells, *J. Bas. and Environ. Sci.,* **2:** 36-51.

Priyanka, S., E.E. Eno, O.O. Lukman, I.B. Obot and M.A. Quraishi (2016). Electrochemical, theoretical and surface morphological studies of corrosion inhibition effect of green naphthyridine derivatives on mild steel in hydrochloric acid, *J. Phys. Chem C,* **120(6):** 3408-3419.

Quraishi, M.A., J. Rawat and M. Ajmal (2000). Dithiobiurets: a novel class of acid corrosion inhibitors for mild steel, *J. Appl. Electrochem.,* **30(6):** 745-751.

Sudhish, K. Sh. and A.Q. Mumtaz (2012). Effect of some substituted anilines-formaldehyde polymers on mild steel corrosion in hydrochloric acid medium, *J. Appl. Polym. Sci.,* **124(6):** 5130-5137.

Taghried, A.S., A.S. Khalida and K. Sh. Jawad (2019). Electrochemical and Computational Studies forMild Steel Corrosion Inhibition by Benzaldehydethiosemicarbazone in Acidic Medium, *Port. Electrochim. Acta,* **37(4):** 241-255.

Zainab, M., W. Mokhalad, N. Amel and S. Balasubramanian (2016). Identification of organic compounds in standardized ethanolic extract of OLEA European (Olive leaves) using GCMS, *ejpmr.,* **3(8):** 520-529.